

Available online at www.sciencedirect.com

Procedia Engineering 10 (2011) 2572–2578

Engineering
Procedia

ICM11

Tensile Strength of Spinnable Multiwall Carbon Nanotubes

N. Khandoker^{a, b,*}, S.C. Hawkins^b, R. Ibrahim^a, C. P. Huynh^b, F. Deng^c^a Department of Mechanical and Aerospace Engineering, Monash University, Victoria, Australia.^b CSIRO Materials Science and Engineering, Bayview Avenue, Clayton Victoria 3168, Australia.^c Graduate School of Frontier Sciences, University of Tokyo, Tokyo, Japan.

Abstract

Individual multi walled Carbon Nanotubes (CNTs) exhibit exceptional strength and stiffness. However, large scale constructs of directly spinnable CNTs (such as yarns) has reached only a few percent of their potential. To improve their performances in such scale, it is important to understand the stress-strain characteristics and failure modes of individual CNTs. This paper reports the experimental tensile strength of spinnable multiwalled carbon nanotubes (MWNT). These experiments were conducted using a nano tensile testing stage inside Scanning Electron Microscope (SEM) chamber. An Atomic Force Microscope (AFM) tip with known force constant was used as a nano manipulator and as a force transducer to measure the desired mechanical properties. Transmission Electron Microscope (TEM) images were used to accurately measure the diameter of CNT samples. The fracture strength was calculated using the determined applied force and the diameter of the CNT. Fracture strength in relations to number of failed walls, pullout (sword/sheath) behaviour and angle of stress are studied. It was found that the tensile strength of the tested spinnable CNTs were at least 20 to 90 Gpa with a mean value of 48 Gpa considering a solid cross sectional area.

© 2011 Published by Elsevier Ltd. Open access under [CC BY-NC-ND license](http://creativecommons.org/licenses/by-nc-nd/3.0/).
Selection and peer-review under responsibility of ICM11

Keywords: Carbon nanotube; tensile strength; spinnable MWNT

1. Introduction

The structure of CNTs promises exceptional properties of strength, stiffness, conductivity, connectivity, surface area, physical and chemical stability for applications ranging from single nano tube based electronics to elevator cables to orbit, from bio-sensors to composites for aerospace and automotive structures[1]. As a pure bulk material, CNTs are ideally suited to forming ultra-high strength yarns for carrying load and electrical current carrying applications. In composites, fibrous material is generally used as reinforcement fillers. The high aspect ratio and physical properties of CNTs make them an obvious choice for composites. However, neither pure bulk nor composite applications, aimed at exploiting their strength, have succeeded in demonstrating this potential at a macroscopic scale. The reasons for this may lie in theoretical strength of the CNTs, the way in which real individual CNTs fail

* Corresponding author.

E-mail address: Khandoker.Noman@monash.edu

and the mechanisms by which CNTs interact with each other and the surrounding matrix. Hence, testing of carbon nanotubes under tensile load and analysing their responses have been the focus of many experimental and theoretical studies.

Direct measurement of carbon nanotube strength and elastic modulus presents major challenges due to the extremely small forces and displacements involved. The small dimensions of CNTs, with diameters in the nanometre range and lengths in the order of hundreds of microns, impose severe constraints on how they can be seen and handled. Together these difficulties have limited the progress in testing and understanding this material.

Theoretical studies of the CNT structure predicted [2, 3] strength and modulus in the vicinity of 100 GPa and 1 TPa respectively and this is broadly confirmed by practical measurements of isolated SWNTs and MWNT outer shells. Initial estimates of SWNT tensile strength were deduced from tests of small bundles and produced values of 45 GPa with 5.8% strain [4] and 22.2 GPa from a rope of 3.6 GPa strength [5]. Ruoff et al. [6] developed a model to calculate the strength of SWNT at the perimeter of ropes, observing a strain of 2–13% with mean strength and modulus of 30 GPa and 0.32 to 1.47 TPa respectively. Individual MWNTs were observed to have strength and modulus of 11 to 63 GPa and 0.27 to 0.95 TPa respectively [7]. In-situ TEM study by Wang et al. [8] reported modulus of 1.2 TPa for arc discharge CNTs and 23–32 GPa for pyrolysis produced CNTs. This suggests that the synthesis and processing of CNTs were important factors for their mechanical characteristics.

More recently double (DWNT) and triple (TWNT) wall CNTs are reported to have strength and modulus of 13–46 GPa and 0.73–1.33 TPa respectively with a strain of 1.5–4.9% [9]. However, TEM based analyses yield somewhat higher strengths of 150 GPa (modulus of 0.9 TPa) [10] and 100 GPa [11]. Most recently another in-situ TEM study validating the effect of CNT defects on strength reported values from 25 to 102 GPa [12]. This range reflects the difficulty in performing the measurements and hence their limited number, and the variability of the samples used. To date these have mainly been samples supplied by third parties, and often have been heavily modified during purification processes.

Macroscopic materials such as pure CNT yarns and composites have only exhibited a fraction of the reported strengths. Pure CNT yarn is one of the most direct means of utilising the fibre strength at the macroscopic scale. CNT yarn can be directly spun from the growth substrate and hence retain their purity by avoiding chemical purification process. But until now these yarns have achieved only 2% of their constituent's potential strength valued around 0.5 to 2.5 GPa [13–15]. There are occasional reports of higher values [16] but nothing approaching the theoretical value of 100 GPa. In order to more nearly achieve the potential strength of this material, it is essential to demonstrate that the constituent CNTs are as strong as necessary, and to understand and optimise their modes of failure and load transfer. Hence, it is pertinent to consider not only the average strength of CNTs but also their strength distribution in the analysis and prediction of yarn strength. This paper reports the strength analysis of CNTs grown specifically to be directly spinnable into a yarn from the growth substrate.

2. Experimental details

2.1 Sample preparation:

The spinnable MWNTs used in this study were grown as a forest on silicon wafer by chemical vapour decomposition (CVD) process. This used semiconductor grade Si substrates, with a thermal oxide layer of thickness 50 nm and an iron catalyst coating of 2.5 nm deposited by e-beam evaporation. A 44 mm id quartz reactor was fed with an acetylene concentration of 2.4% in helium (25 sccm in 1000 sccm He) with a running time of 10 minutes and temperature of 680 °C. More details of this process are published elsewhere [17].

The vertically aligned MWNTs in the forest can be drawn into a web of CNTs which is the major assessment indicator for the spinnability property of carbon nanotubes [18]. The web was initiated with the sharp edge of a scalpel plunged down into the forest and then by pulling it away horizontally. The CNTs from the forest string out behind the scalpel and hold together without any presence of binding agent.

To prepare the test samples, the CNT web was laid on to a thin layer of graphite paint. A second layer of paint was placed over the web and allowed to dry. The samples were then oven dried at 350 °C for 30 minutes to fully dry the paint and evaporate the polymer binder. The CNT web and the graphitic film then formed a very thin layer which was torn apart leaving the spinnable MWNTs protruding from the edge. The torn film was placed into the experimental setup and was used as the source of the tested MWNT specimens.

2.2 Experimental setup:

Here, we extend the use of the method previously proposed by [7, 19] to measure the strength of multiwalled carbon nanotubes. MWNTs were tensile loaded in a nano physical testing stage which comprises two piezoelectric actuators and three ultrasonic motors. The movement of this stage can occur in two phases: “coarse movement” and “fine movement”. The coarse movement in X, Y and Z directions can be attained by ultrasonic linear friction motors with carbon fibre shafts. The fine movement was achieved with close ply stack type piezoelectric actuators in X and Z directions and an extremely stable variable dc power supply to maintain or vary positions. An Atomic Force Microscope (AFM) tip was attached to the X-piezo. The CNT sample and the reference AFM tip were placed on the Z-piezo. The coarse (X, Y and Z directions) and fine (X and Z directions) movements were used to move the AFM tip to collect and test the CNT. The whole nano physical testing stage was operated inside a Field Emission Scanning Electron Microscope (FESEM) chamber (Philips XL30). The electron beam energy of 2 keV in the SEM was kept to a minimum level to avoid accumulation of amorphous carbon on to the test samples. Each experiment was recorded on video, and the data was analysed after conversion of the video frame images to computer files.

2.3 Tensile testing process:

The working AFM tip, attached to X-piezo, acted as a nano manipulator as well as a force sensor. As a nano manipulator the AFM tip was used to collect the CNT specimen from the sample. The working AFM tip was calibrated against a reference AFM tip mounted on the stage which was pre-calibrated by measuring the resonant frequency of the cantilever beam and combining it with the Euler – Bernoulli beam theory [20, 21]. To calibrate the working AFM cantilever, it was positioned on to the reference AFM cantilever and the deflections of both of them were recorded at several positions. The force applied to them will be equal in magnitude but opposite in direction. Therefore, knowing the spring constant of the reference AFM tip beforehand and measuring the deflections of both the AFM tips allowed the spring constant of the working tip to be calculated. In this process it was assumed that the spring constants of both cantilevers were not altered either by the direction of the force or by the small displacement used in the experiment. The spring constant of the utilized working AFM cantilever was found to be 0.29 N/m for the first experiment and 0.42 N/m for the second.

Attachment of individual MWNTs to the probe was achieved by in situ deposition of amorphous carbon through extended scanning by the electron beam of the microscope. After manoeuvring the AFM tip to touch a single CNT, the beam was focussed only on the area of contact for several minutes. The electron beam decomposed traces of carbonaceous vapour in the SEM environment which accumulated as carbon on the sample as it rests on the probe, hence welding it firmly in place. Each specimen was then gradually stress-loaded through the probe by retracting the piezo actuator while observing the process by SEM. Fibres either pulled free from the graphite film, in which case they were then transported to and welded onto a TEM grid which is also mounted on the Z piezo for testing; or the fibres snapped, in which

case the load to break was recorded. If sufficient length of fibre remained on the AFM tip after the initial break, the distal end was positioned on the TEM grid, welded and the fibre tested again. By this means and by repositioning the broken pieces, one fibre was successfully tested in a total of 16 trials.

A video record was made of each test and then used to measure displacement of the probe up to failure of the CNT. Hence, the AFM probe used in these experiments acted as a force transducer which measures force as a function of displacement. The video capture included an 8-frame averaging function to reduce noise. This superimposed image (Figure 1a) together with the data bar provided by the SEM gives the required displacement data. The force constant of the AFM cantilever probe and the CNT diameter is used for calculating the strength of the CNT.

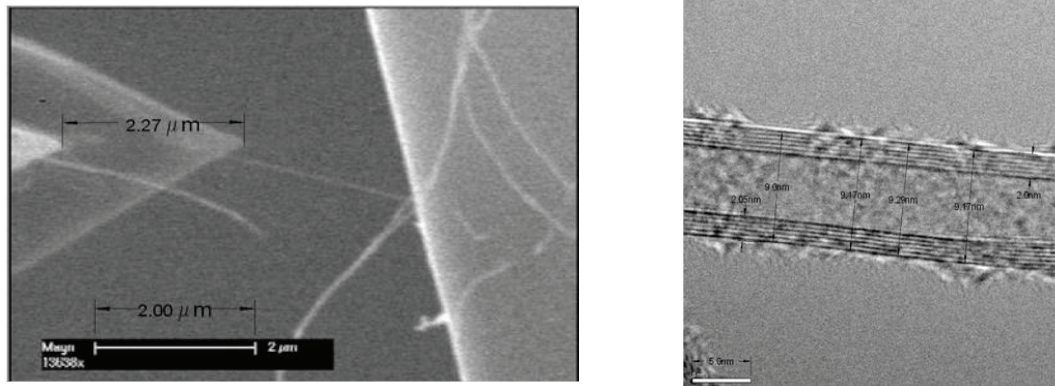


Figure 1: (a) Superimposed video frames for force measurement (b) Repeated measurement of CNT diameter.

2.4 Diameter measurement:

A Transmission Electron Microscope (FEI Technai G2) was used to estimate the diameters of the CNTs used. Due to the amount of amorphous carbon accumulating on the CNTs attached to the TEM grid used, it was difficult to place the samples on TEM grid and then transfer them from the SEM to the TEM. Therefore, diameters were estimated by measuring many pristine CNTs taken at random from the same forest used in preparing specimens for the experimental strength tests. The electron beam energy during TEM imaging was kept at a minimum level to reduce the damage of samples and to avoid amorphous carbon accumulation on them.

3. Results and discussion:

3.1 Diameter distribution:

A number of samples were measured to obtain the diameter distribution of the tested MWNTs for this purpose. First it is presented that the nanotube diameter measurement method is reliable and can be repeatedly used for this purpose. The measurement was taken using a sample image as presented in Figure 1b below. From the presented figure it can be seen that the measurement on the same sample are quite repeatable with mean outer diameter of 9.16 nm and standard deviation of 0.12. The data bar was used in this measurement as a reference dimension. But the constant wall spacing (0.34 nm) can also be used as the reference dimension. It can be observed from the image that the sample had 6 walls. Hence, the wall thickness should be 2.04 nm which can also be used to ensure the correct calibration of the data bar from the TEM. The outer diameter of individual CNTs within these samples were found to be 10.77 nm with standard deviation of ± 1 .

3.2 Strength of spinnable nanotubes

As already mentioned before, the main focus of this paper is to experimentally determine the axial tensile strength of spinnable CNTs. As a first approximation, the cross sectional area of the tested specimen was assumed to be of a solid cylindrical bar. This assumption provides the basis for calculating the most

conservative or practical limiting strength of a MWNT but is relatively sensitive to the diameter measurement as it depends only on the cross sectional area of the CNT. At the other extreme is to consider only the outer shell circumferential area (hollow cylinder) of a MWNT for its load bearing capability[7]. This calculates the highest possible strength value for MWNTs. It is less sensitive to diameter measurement as it depends mainly on the wall circumference, the wall thickness being known.

To gain fundamental understanding of the strength characteristics of spinnable MWNT sequential testings of a single specimen was performed. A spinnable MWNT was tested 16 times by repeatedly re-capturing and welding the broken pieces (ie not always by breaking the remaining length on the AFM tip as it became progressively shorter). Figure – 3 shows the results of these sequential tensile loading experiments binned at 2 Gpa intervals (0.29 N/m AFM spring constant). Of the four lowest values, two are attributable to the CNT being stressed at an angle, one example of which is illustrated in Figure 1, one is attributable to a fragment of another CNT attached to the tested CNT where the tested sample was broken. No attribution is made for the other low value. The remaining values are clustered into one large group ranging with a mean of ~14.0 GPa (standard deviation of 1.7) and a cluster of three high values with a mean of 23.8 GPa (standard deviation of 1.9).

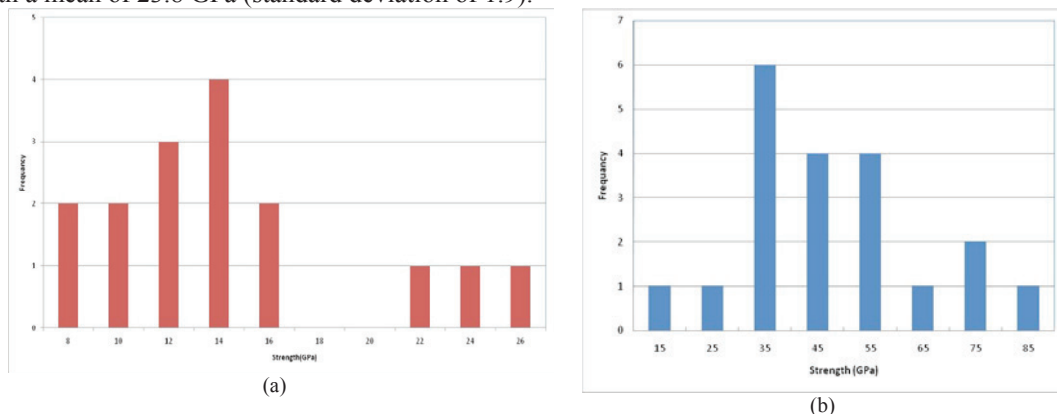


Figure 2: (a) Sequential tensile test results of spinnable nanotube (b) Individual tensile test results of spinnable nanotube

Table i: Sequential test data spread

| Bin (MPa) | 8 | 10 | 12 | 14 | 16 | 18 | 20 | 22 | 24 | 26 |
|--------------------------------|------|------|-------|-------|-------|----|----|-------|-------|-------|
| Mean among bin values (MPa) | 8.57 | 9.92 | 12.16 | 14.38 | 16.06 | - | - | 22.21 | 23.36 | 25.85 |
| Std deviation among bin values | 0.12 | 0.28 | 0.9 | 0.72 | 0.79 | - | - | - | - | - |

Table ii: Individual tests data spread

| Bin (MPa) | 15 | 25 | 35 | 45 | 55 | 65 | 75 | 85 |
|--------------------------------|----|----|-------|-------|------|----|------|----|
| Mean among bin values (MPa) | 11 | 27 | 34.17 | 43.75 | 52.5 | 63 | 74.5 | 80 |
| Std deviation among bin values | - | - | 2.31 | 3.77 | 3.31 | - | 2.12 | - |

It is notable here that the sequentially tested MWNT specimen was assumed to be defect free and pristine in nature. Therefore, the spread in test results may be caused either by measurement errors or due to variability of the tested specimen. To reduce any occurrences of measurement errors the experiments were performed with extreme cautions. The variability of the MWNT specimen can be interpreted from the fundamental understanding of the structure, interaction and load transfer mechanisms between the MWNT walls.

A multiwall nanotube is an array of hollow single-wall nanotubes arranged concentrically in symmetric positions with a repeat spacing of 0.34 nm. In each of these concentric layers, the bondings between carbon atoms are covalent in nature, but there are no physical bondings between the walls. The interactions between the nanotube walls are due to Van der Waals forces. For the test configuration used in this study, the MWNT specimen was welded by amorphous carbon deposition on to the outer most wall. Hence, in this test configuration the outer layer carried almost the entire load. The outer wall of the tested specimen was 10.77 nm in diameter. The remaining geometric parameters involved are the length and the number of walls in the tested specimen. The effect of gauge length on tensile strength characteristics have not yet been considered in this study which may cause scattering in data due to defect frequency. Therefore, the observed variability in these results can be attributed to the load carrying capacity of multiple walls of the MWNT specimen. For a 10.77 nm nanotube the second wall would have a diameter of around 10.09 nm. These variations in nanotube diameters affect the strength of MWNT. Therefore, a group of MWNT specimen with different diameters were tested individually to evaluate this effect.

Figure 2(b) presents the strength distribution of spinnable MWNTs which were individually tested. The mean and the standard deviation values are also provided in Table ii. The lowest value of 11 GPa from these tests are due to occurrence of separation of the test specimen from the AFM tip. As discussed previously, the frequency in the lowest strength value represents the breakage of the outer- most wall only. In this case the strength valued in range from 30 GPa to 40 GPa. The variations in the peak values between the two sets of experimental results depict the effect of variation of the diameter. Further scheme of models for describing such effects are needed to be developed.

4. Conclusion:

In summary, the testing procedure for spinnable nanotubes was presented in this paper. A conservative approach for nanotube strength calculation was utilized. The data from sequential testing of a single specimen of MWNT was used to model the results. It was found that the strength of spinnable nanotube to be in the range of 20 to 90 GPa with a mean of 48 GPa considering the solid cylinder assumption. But when they were considered as a hollow cylinder their strength was in range of several hundreds of GPa with a mean value of 378 GPa.

5. References:

- [1] Baughman, R.H., A.A. Zakhidov, and W.A.d. Heer, *Carbon Nanotubes--the Route Toward Applications*. Science, 2002. **297**: p. 787 - 792.
- [2] Belytschko, T., S.P. Xiao, and R. Ruoff, *Effects of Defects on the Strength of Nanotubes: Experimental-Computational Comparisons*. Los Alamos National Laboratory preprint.
- [3] Natsuki, T. and M. Endo, *Stress simulation of carbon nanotubes in tension and compression*. Carbon, 2004. **42**: p. 2147-2151.
- [4] Walters, D.A., et al., *Elastic strain of freely suspended single-wall carbon nanotube ropes*. APPLIED PHYSICS LETTERS, 1999. **74**(25): p. 3803-3805.
- [5] Li, F., et al., *Tensile strength of single-walled carbon nanotubes directly measured from their macroscopic ropes*. APPLIED PHYSICS LETTERS 2000. **77**(20).
- [6] Yu, M.-F., et al., *Tensile Loading of Ropes of Single Wall Carbon Nanotubes and their Mechanical Properties*. Physical Review Letters, 2000. **84**(24): p. 5552.
- [7] Yu, M.-F., et al., *Strength and Breaking Mechanism of Multiwalled Carbon Nanotubes Under Tensile Load*. Science, 2000. **287**(5453): p. 637-640.

- [8] Wang, Z.L., et al., *Mechanical and electrostatic properties of carbon nanotubes and nanowires*. Materials Science and Engineering: C, 2001. **16**(1-2): p. 3-10.
- [9] Wei, X., et al., *Tensile Loading of Double-Walled and Triple-Walled Carbon Nanotubes and their Mechanical Properties*. The Journal of Physical Chemistry C, 2009. **113**(39): p. 17002-17005.
- [10] B.G. Demczyk , et al., *Direct mechanical measurement of the tensile strength and elastic modulus of multiwalled carbon nanotubes*. Materials Science and Engineering A, 2002. **334**: p. 173-178.
- [11] Peng, B., et al., *Measurements of near-ultimate strength for multiwalled carbon nanotubes and irradiation-induced crosslinking improvements*. Nat Nano, 2008. **3**(10): p. 626-631.
- [12] Ming-Sheng Wang , Dmitri Golberg , and Y. Bando, *Tensile Tests on Individual Single-Walled Carbon Nanotubes: Linking Nanotube Strength with Its Defects*. Advanced Materials, 2010: p. 1-5.
- [13] Kai Liu, et al., *Carbon nanotube yarns with high tensile strength made by a twisting and shrinking method*. Nanotechnology, 2010. **21**: p. 1-8
- [14] Atkinson, K.R., et al., *Multifunctional carbon nanotube yarns and transparent sheets: Fabrication, properties, and applications*. Physica B: Condensed Matter, 2007. **394**(2): p. 339-343.
- [15] I J Beyerlein, et al., *Scale and twist effects on the strength of nanostructured yarns and reinforced composites*. Nanotechnology, 2009. **20**: p. 485702 (1-10).
- [16] Vilatela, J.J., J.A. Elliott, and A.H. Windle, *A Model for the Strength of Yarn-like Carbon Nanotube Fibers*. ACS Nano, 2011: p. null-null.
- [17] Chi P. Huynh and S.C. Hawkins, *Understanding the synthesis of directly spinnable carbon nanotube forests*. Carbon 2010. **48**: p. 1105-1115.
- [18] Huynh, C.P., et al., *Evolution of directly-spinnable carbon nanotube growth by recycling analysis*. Carbon (Inpress), 2011.
- [19] Deng, F., T. Ogasawara, and N. Takeda. *Microscopic dynamic observation and experimental characterisation of carbon nanotubes Poly ether ether ketone composites*. in *Twelfth US-Japan conference on composite materials*.
- [20] Cleveland, J.P., et al., *A nondestructive method for determining the spring constant of cantilevers for scanning force microscopy*. Rev. Sci. Instrum. , 1993. **64**(2): p. 403-405.
- [21] Sadara, J.E., J.W.M. Chon, and P. Mulvaney, *Calibration of rectangular atomic force microscope cantilevers*. Review of Scientific Instruments 1999. **70**(10).